Physica Medica 57 (2019) 88–94

Contents lists available at ScienceDirect

Physica Medica

journal homepage: www.elsevier.com/locate/ejmp

Original paper

Optimized neuron models for estimation of charged particle energy deposition in hippocampus

Munkhbaatar Batmunkh[a,*], Svetlana V. Aksenova[a], Lkhagvaa Bayarchimeg[a], Aleksandr N. Bugay[a,*], Oidov Lkhagva[b]

[a] Laboratory of Radiation Biology, Joint Institute for Nuclear Research, Dubna 141980, Russia
[b] Division of Natural Sciences, National University of Mongolia, Ulaanbaatar 210646, Mongolia

ARTICLE INFO

Keywords:
Hippocampal neuron models
Monte Carlo track simulation
Spike frequency
Neural network

ABSTRACT

The study of evaluating radiation risk on the central nervous system induced by space-born charged particles is very complex and challenging task in space radiobiology and radiation protection. To overcome computational difficulties in this field, we developed simplified neuron models with properties equivalent to realistic neuron morphology. Three-dimensional structure and parameters of simplified and complex neuron models with realistic morphology were obtained from the experimental data. The models implement uniform random distribution of spines along the dendritic branches in typical hippocampal neurons. Both types of models were implemented and tested using Geant4 Monte Carlo radiation transport code. Track structure simulations were performed for ion beams with typical fluxes of galactic cosmic rays expected for long-term interplanetary missions. The distribution of energy deposition events and percentage of irradiated volumes were obtained to be similar in both simplified and realistic models of pyramidal and granule cells of the rat hippocampus following irradiation. Significant increase of computational efficiency for detailed microdosimetry simulations of hippocampus using simplified neuron models was achieved. Using designed neuron models we have constructed 3D model of the rat hippocampus, including pyramidal cells, mature and immature granular cells, mossy cells, and neural stem cells. Computed energy deposition in irradiated hippocampal neurons following a track of iron ion suggests that most of energy is accumulated by dense population of granular cells in the dentate gyrus. Proposed approach could serve as a complementary computation technique for studying radiation-induced effects in large scale brain networks.

1. Introduction

Estimation of radiation damage to the central nervous system (CNS) has been attracting significant attention in space radiobiological research related to radiation protection for astronauts during space travel beyond the Earth magnetosphere [1–3]. Brain neurons are mostly non-dividing and have highly variable cell morphology. Most neurons have soma, axon, and multiple dendrite branches, which contain numerous dendritic spines ensuring synaptic connections between different cells. They dendrites form tree-like arborization around the neuron, which main purpose is to receive and integrate electrochemical signals heading towards the soma, while axon sends information away from the soma. Known effects of charged particles traversing the cells of central nervous system (CNS) include degradation of dendrite tree morphology [2,4] and disturbance of electrochemical processes governing synaptic transmission [5,6]. This earliest radiation injury to individual neurons can result in long-term effects including various impairments of behavior, memory and other cognitive deficits [3,7]. Also, the biological efficiency of heavy ions present in galactic space radiation are several times higher than for protons [8].

The analysis of recent experimental studies at particle accelerators with energetic protons and heavy ions suggests that the hippocampus is one of the most sensitive regions of the CNS under irradiation [1,6]. The hippocampal neurons organized in various neural networks play an important role in learning, memory consolidation as well as in the processing of the information received simultaneously from diverse sources. Rodent hippocampal neurons are among the most intensively studied neural systems. In the rat hippocampus, there are two main types of principal neurons: population of about 1.2 million granule cells in dentate gyrus (DG) region and population of about 0.6 million

* Corresponding authors.
E-mail addresses: batmunkh@jinr.ru (M. Batmunkh), kgyr@mail.ru (S.V. Aksenova), bayarchimeg@jinr.ru (L. Bayarchimeg), bugay@jinr.ru (A.N. Bugay), dorjtoinol@gmail.com (O. Lkhagva).

https://doi.org/10.1016/j.ejmp.2019.01.002
Received 10 August 2018; Received in revised form 29 December 2018; Accepted 1 January 2019
Available online 03 January 2019

pyramidal cells in cornu ammonis (CA3/CA1) region, respectively [9]. These neurons are characterized by complicated dendritic trees with a great number of branches.

Although the precise mechanisms of radiation-induced injury in CNS structures still remain unclear, the development of mathematical and computational approach of brain cells irradiation with the use of Monte Carlo track structure techniques seems to be an extremely important task in the analysis of the neuro-radiobiological effects of accelerated charged particles at molecular and cellular levels. First steps performed in this direction [10–14] allowed to estimate dose distributions and dendrite degradation in compartmental models of single neurons and small-scale neural networks. Present work focuses at designing the optimal models of hippocampal neurons to establish a basis for simulation of networks several orders larger than in previous papers followed by energy deposition in particle tracks.

2. Methods

In the present work, simplified models of a DG granule and a CA3/CA1 pyramidal cell were constructed from complex models of realistic rat hippocampal neurons whose morphologies are available from Claiborne archive at the NeuroMorpho.Org repository [15]. In our model the soma is represented by a single ellipsoid and the segments of the dendritic branches are represented with combination of cylindrical compartments. The distribution of spines along the dendritic branches was simulated in accordance to the experimentally measured spine density [16,17]. Each spine is represented by joint cylindrical and spherical solids perpendicular to the dendrite surface and randomly placed on dendrites according to normal (Gaussian) distribution with given density of 12.8 ± 1.4 (DG) and 10.5 ± 1.2 (CA3/CA1) spines per 10 μm. The spine sizes were generated randomly from a Poisson distribution in accordance with the measured diameter (0.28 ± 0.16 μm) and length (0.36 ± 0.17 μm) of spine neck and diameter (0.48 ± 0.21 μm) of spine head [18,19]. It should be noted, that both realistic and simplified neuron models contain dendritic segments and spines varying in number, diameter and length. However, the overall volume and spine density of simplified neuron models are similar to the realistic neuron models. This means that the diameter of the segments in simplified cells has to be greater than in the realistic cells. Such a design is also intended to preserve correct electrical properties of neuron compartments, as it is usually done in the computational neuroscience [20]. This was the one of the criteria to select the compartment sizes. The major morphological parameters of simulated neurons are presented in Table 1. Sample 3D geometries of both neuron models are illustrated in Fig. 1.

With the use of simplified neuron models, we have designed 3D model of the rat hippocampus, scaled about 1:100 with respect to real structure. The model contains different types of neural cells - CA3/CA1 pyramidal cells and DG granule cells, as well as interneurons and neural stem cells. The dorsal view of hippocampus is depicted in Fig. 2c. The reconstruction of the hippocampus structure is based on the digitally traced cytoarchitectonic segmentation of rat hippocampal regions and details of structural properties are reported in the literature [21]. The model illustrated in Fig. 2 contains populations of 11960 DG granule cells, 3480 CA1 pyramidal neurons and 2401 CA3/CA2 pyramidal neurons, 496 mossy cells in hilus (HMC), 560 DG immature neurons (IMN) and 110 neural stem cells (NSC) in the subgranular zone. The neurons are located in the hippocampal regions within the water box with overall dimensions of 4608 × 7106 × 1000 μm [9,22]. A single neural stem cell, immature neuron and hilar mossy cell are represented with volumes of 3284.4 ± 468.1 μm^3, 6786.7 ± 1206.4 μm^3 and 6328.7 ± 1513.1 μm^3 [22]. The number of segments was 5, 7, and 9, respectively. For such low numbers of segments and cell population the design of simplified models for NSC, IMN and HMC neurons was reasonless.

Table 1
Geometrical parameters of principal neuron components in the rat hippocampus.

	Volume (μm^3)		Number of segments	
Model	Realistic	Simplified	Realistic	Simplified
		CA1 pyramidal cell		
Soma	2234.8 ± 321.6		1	
Dendrites	27384.7 ± 5992.8	26951.2 ± 6078.3	2643 ± 186	63
Spines	3564.4 ± 667.8	3387.9 ± 786.4	14687 ± 3894	3782 ± 1874
Total	33184.9 ± 6982.3	32573.9 ± 7186.3	17331 ± 4080	3846 ± 1874
		DG granule cell		
Soma	912.3 ± 207.3		1	
Dendrites	8849.5 ± 2381.3	8167.2 ± 1967.2	567 ± 263	8
Spines	801.3 ± 198.5	758.9 ± 227.2	3897 ± 304	1198 ± 231
Total	10563.1 ± 2787.1	9838.4 ± 2401.7	4465 ± 567	1207 ± 231

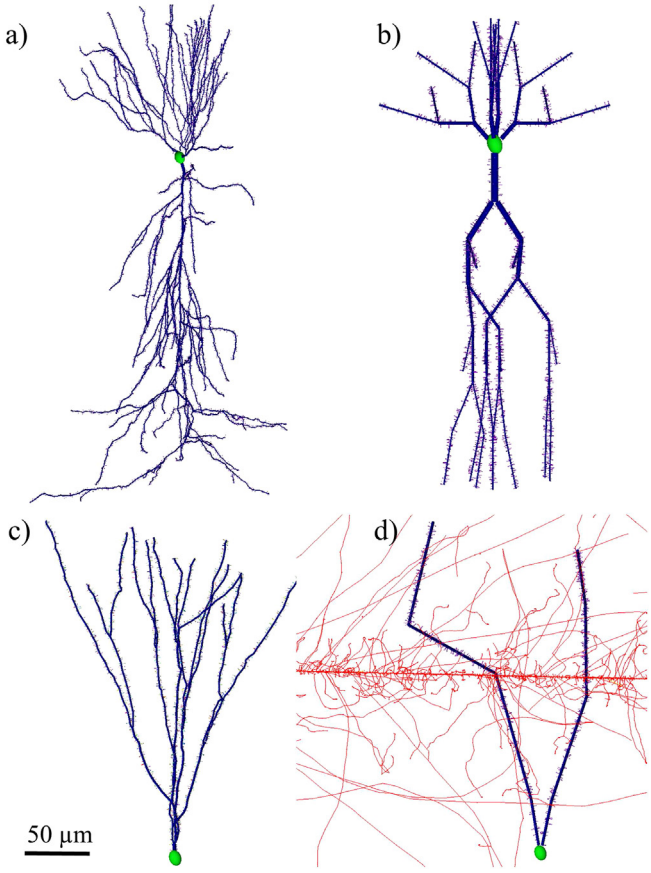

Fig. 1. Samples of three-dimensional realistic and simplified models of a pyramidal (a, b) and granule cell (c, d) with dendritic spines. An example of simulated track structure (red online, thin long lines in print) of single 600 MeV/u ^{56}Fe ion traversing simplified model of a granule cell (d).

Track structure simulations of charged particles passing through the neuron were performed using the Geant4/Geant4-DNA (v.10.4) Monte Carlo radiation transport code [23–26]. The Geant4 condensed electromagnetic models are used outside the neuron structure and Geant4-DNA discrete physico-chemical models are activated inside the neuron structure. The cutoff transport energy of secondary electrons within neuron volume was used with the default value (7.4 eV). Particle transport within neuron structures were simulated using the “neuron” example included in the Geant4-DNA (v.10.4). The details of neuron geometry implementation and Geant4-DNA classes used for the simulation of particle transport were described in our previous works [10,12,13]. The distributions of energy deposition events were

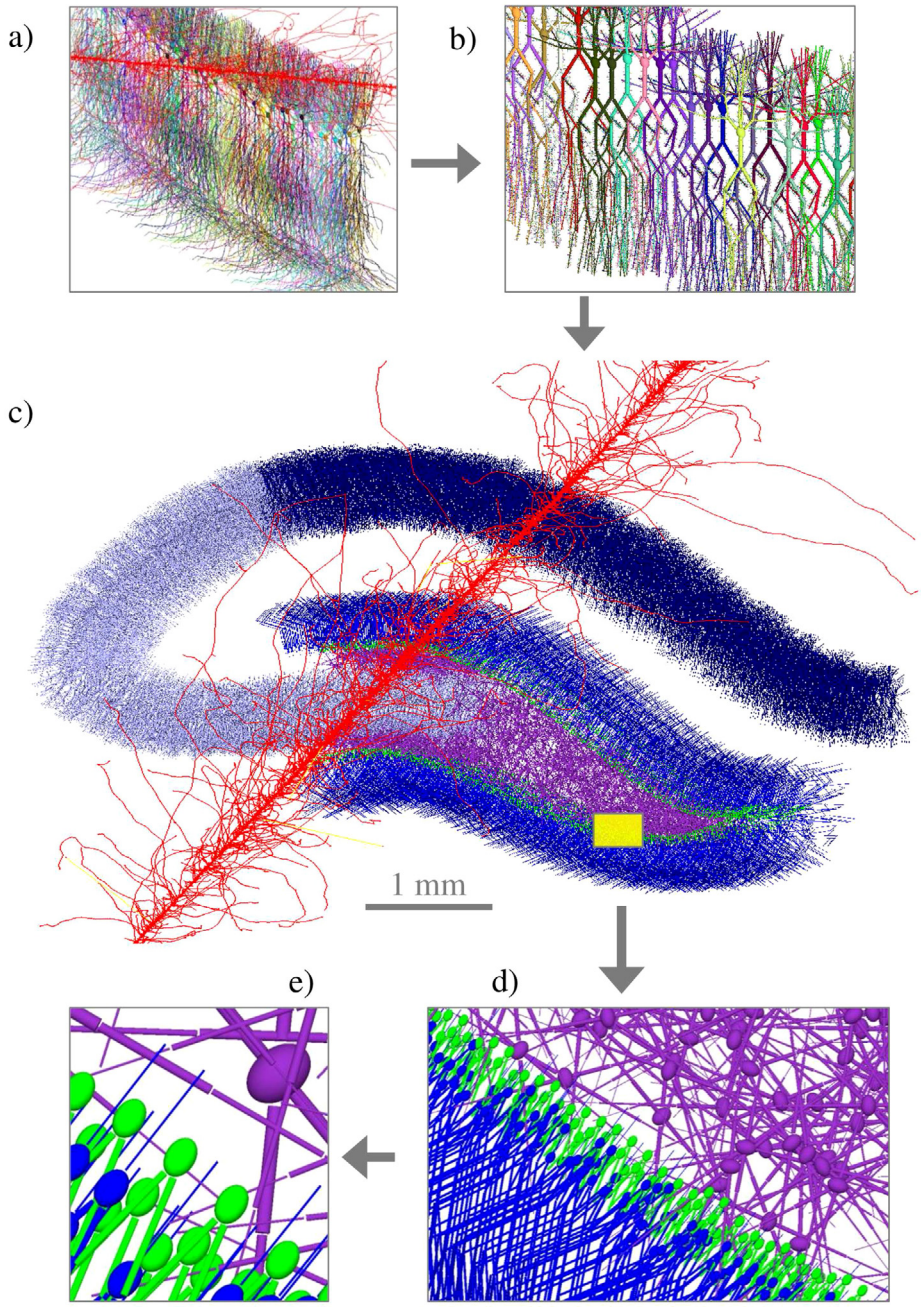

Fig. 2. A sample three-dimensional representation of different neurons in the rat hippocampus which are traversed by single track of ^{56}Fe ion. An example of realistic (a) and simplified (b) networks of individual pyramidal neurons in the CA1 region. The center panel (c) shows the dorsal view of the 3D model of hippocampus; the inserted panel depicts a close-up view of the selected region (the yellow square). The DG granule cells are highlighted in blue, neurons in the subgranular zone – green, mossy fibers in the hilus – purple, CA1 pyramidal neurons – dark blue, and CA3/CA2 pyramidal neurons – light blue. The track structure of 600 MeV/u ^{56}Fe ion is given in red. (For interpretation of the references to colour in this figure legend, the reader is referred to the web version of this article.)

computed for beams of 600 MeV/u ^{56}Fe ions with fluences of $3.2{\cdot}10^5$ particles/cm^2 and $6.7{\cdot}10^6$ particles/cm^2. Such particles are present in the spectra of galactic cosmic rays [27].

The irradiation of the rat hippocampus model (Fig. 2) was simulated in water box with overall dimensions of 4608x7106x1000 μm. Particles were generated from the box edges and randomly directed inside the box, containing the hippocampus, and then the energy depositions in track structures of primary and secondary particles were computed for each type of irradiated neurons.

All computations were performed on a server with Intel Xeon Gold 6136 Processor (24.75 M Cache, 3.00 GHz base, 3.70 GHz turbo). At the end of each simulation, the information about the CPU time and memory used was summarized. For a given number of neurons in a network we divided the average memory used to simulate a network composed of realistic cells by the average memory used to simulate a network composed of simplified cells. Obtained ratio can be used as a relative measure of resource consumption. To measure CPU time we have simulated particle tracks in neural networks of 100 cells with composition of realistic or simplified models using single thread computation.

3. Simulation results

3.1. Comparison of realistic and simplified neuron models for calculation of energy depositions

In the first part of our study we have compared the properties of realistic and simplified neuron models for dosimetric applications. Three-dimensional neuron models (see Fig. 1) were irradiated with 600 MeV/u ^{56}Fe ion beams of different fluences. The mean numbers of particle-track traversals across different models of pyramidal and granule neuron are plotted in Fig. 3. The number of particle-track traversals were found to have quite different for realistic and simplified neuron models. In the case of realistic neuron model, numerous

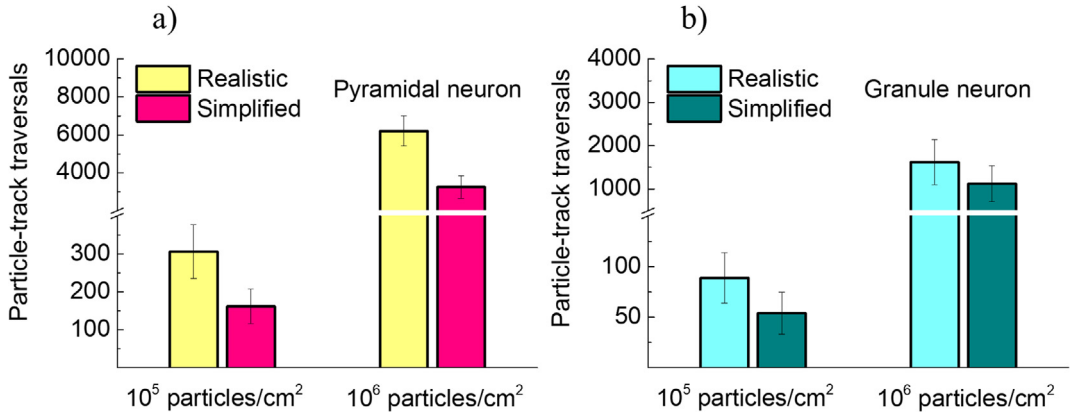

Fig. 3. Mean number of particle-track traversals for the different models of pyramidal and granule neurons (a, b) following the exposure to 600 MeV/u ^{56}Fe ions with fluences of 10^5 particles/cm^2 and 10^6 particles/cm^2. The results are averaged over 10 different neuron morphologies in each case.

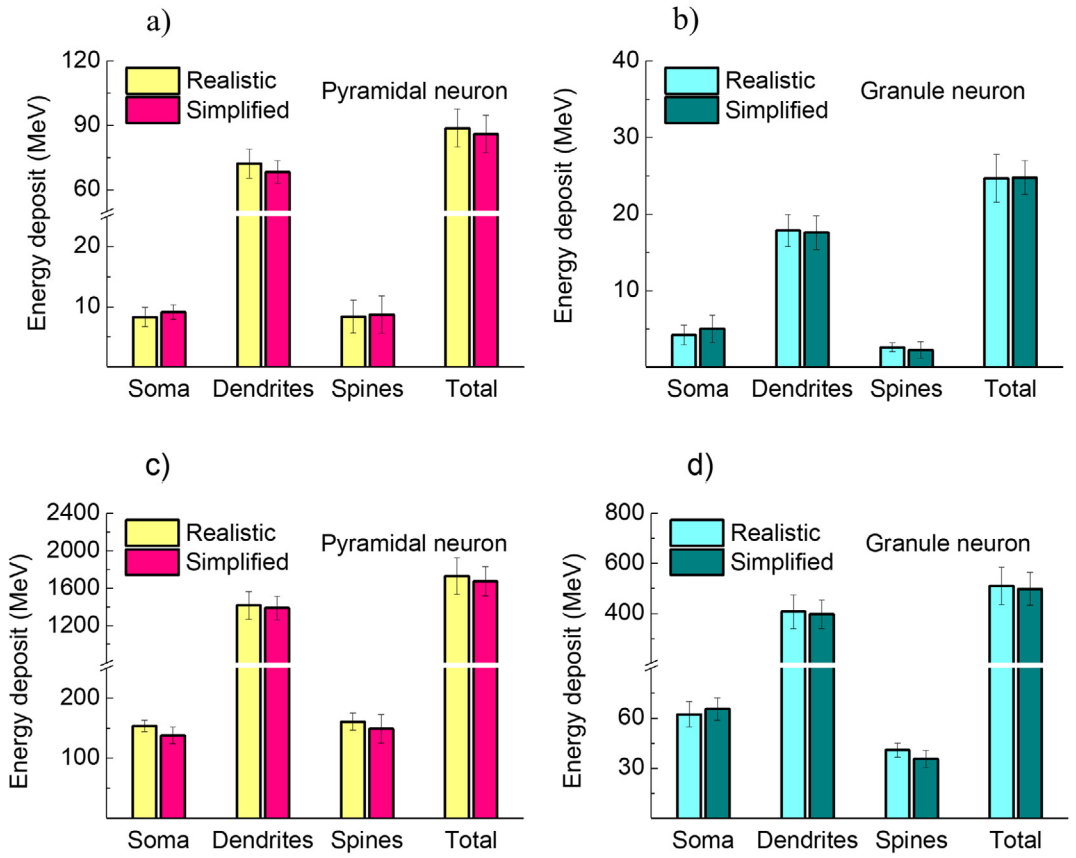

Fig. 4. Total energy deposition in realistic and simplified model of pyramidal (a,c) and granule neuron (b,d) under exposure to 600 MeV/u ^{56}Fe ions with fluences of $3.2{\cdot}10^5$ particles/cm^2 (a,b) and $6.7{\cdot}10^6$ particles/cm^2 (c,d). Corresponding doses to hippocampus will be 0.1 Gy and 2 Gy, respectively.

dendritic branches with thin structure receive large number of hits with smaller amount of energy deposition. On the contrary, in the case of simplified neuron model small number of dendritic branches with larger volumes receive small number of hits with larger amount of energy deposition. Therefore, total energy deposition was obtained to be similar in the soma, dendrites and spines of both realistic and simplified geometries (Fig. 4). The error bars reflect the difference in the energy depositions averaged over 10 different morphologies of realistic and simplified neuron models. Comparison of irradiated volumes show similar results for both the realistic and simplified dendritic models of hippocampal neurons following irradiation with different fluences (Table 2). The difference between realistic and simplified neuron models was rather small in terms of total energy depositions.

3.2. Application of simplified neuron models for the calculation of energy deposition in the rat hippocampus

With the use of simplified neuron models, we have simulated the irradiation of the rat hippocampus model. The mean number of irradiated hippocampal neurons normalized per single track of 600 MeV/u ^{56}Fe particle is plotted in Fig. 5. It is shown that the largest numbers of irradiated neurons are found in the DG region of hippocampus, mostly because DG granule cells constitute the majority of neuron population. On the other hand, the amount of energy deposition in neural stem cells is much smaller than in other types of hippocampal neurons (see Fig. 5b). However, these numbers could be of great importance, because proliferating neural stem cells are the most radiosensitive in

Table 2
Percentage of irradiated volume of soma, dendrites and spines under exposure to 600 MeV/u ^{56}Fe ions with fluences of $3.2{\cdot}10^5$ particles/cm^2 and $6.7{\cdot}10^6$ particles/cm^2. Corresponding doses to hippocampus will be 0.1 Gy and 2 Gy, respectively.

Fluence	$3.2{\cdot}10^5$ particles/cm^2		$6.7{\cdot}10^6$ particles/cm^2	
Model	Realistic	Simplified	Realistic	Simplified
		CA1 pyramidal cell		
Soma	33.3 ± 6.7	35.5 ± 6.2	96.8 ± 3.2	96.5 ± 3.5
Dendrites	96.8 ± 3.2	100	99.8 ± 0.2	100
Spines	23.6 ± 4.0	39.4 ± 4.8	96.4 ± 3.6	99.2 ± 0.8
		DG granule cell		
Soma	29.6 ± 5.1	31.3 ± 5.4	85.7 ± 4.7	81.5 ± 5.8
Dendrites	98.4 ± 1.6	100	100	100
Spines	25.2 ± 5.1	40.2 ± 6.3	97.7 ± 2.3	98.4 ± 1.6

contrast to other more abundant neuron types throughout the hippocampus.

3.3. CPU time and memory usage

Finally, we have estimated computational resources required for the simulations incorporating simple or realistic neuron models.

Monte-Carlo track simulation in Geant4-DNA environment could take a lot of operative memory for targets with a size of hundreds and thousands cells and heavy particles producing great number of physical and chemical events. The total amount of memory used for simulations with different models of hippocampal neurons at the level of single cells and populations is reported in Fig. 6. The amount of used memory increases with the number of neurons for both the realistic and simplified geometries. However, the realistic geometry results in several times higher memory consumption. For a few neurons (1–10), the simulation memory seems to be nearly equivalent for both geometries. But then the ratio between the sizes of memory used for realistic and simple neuron geometries rapidly increases from 1.5 to 5 for pyramidal cells and from 1.2 to 5 for granule cells for the given range of 1–2000 neurons.

The results of CPU time used for single thread computation are presented in Fig. 7. Obviously, Geant4 achieves significant speedup in computation with the implementation of simplified neuron models. Most notable decrease of time (3x) was obtained for DG and CA1 network. In the case of neural stem cells, immature neuron and mossy cells, we did not compare morphology and computation differences, because they have very simple dendritic trees, and also their population in hippocampus is much smaller than granular cells and pyramidal neurons.

4. Discussion and conclusion

To find a way to overcome computational difficulties in radiobioligical studies of large populations of brain neurons, we developed simplified neuron models with smallest number of segments, but functional properties to be equivalent to realistic neuron morphologies. The geometrical structure and electrical properties of simplified and complex neuron models with realistic morphology were based on the experimental data. For the simulations of particle track structure in hippocampal neurons, Geant4 Monte Carlo radiation transport code were used.

The selection of the hippocampal neurons was motivated by the great number of experimental findings supporting the importance of this brain structure in radiation-induced cognitive impairments. Hippocampal neurons are distributed throughout the million-cell networks in DG and CA regions. The dendritic trees of most neuron cells have a complicated spatial composition and accumulates the largest portion of energy deposition compared to the soma [10–14]. In the course of this study we evaluated and compared the distribution of energy depositions in a simplified and realistic model of CA pyramidal and DG granule neurons. According to the simulation results, the differences between realistic and simplified neuron model were found to be very small in terms of total energy depositions in soma, dendritic tree, and the spines distributed along the dendrites. Relative difference between total energy depositions for measured quantities in both types of models typically does not exceed several percent. This result is explained by proper scaling of the neuron geometry, according to which the overall volume and spine density of simplified neuron models are similar to the realistic ones, but the number and the size of segments in simplified neuron models is different than those of the realistic neuron models. Such scaling also insures that correct electrical properties of neuron compartments are reproduced by both types of models.

As a result we achieved significant reduction in computation time and memory consumption using simplified neuron models. For simulations including up to hundred cells differences in computation time and memory consumption were not so evident, but the composition of a neural network containing several hundreds of cells provides acceleration of computation up to ten fold (Fig. 7). Absolute times of simulation were not a real challenge for a modern CPU. However, the operative memory consumption during Monte-Carlo track simulations was significantly reduced (Fig. 6) for neural networks with simple models. For example, simulating population of a thousand neurons requires 32.5 GB of memory for realistic geometry and 6.7 GB for simplified geometry of the pyramidal cell (see Fig. 6). This could bring real benefit for researchers using low- and middle-end desktops.

Thus, we should emphasize that the implementation of the realistic morphology meets difficulties in dosimetric studies of large scale biological neural networks. To demonstrate the possibilities of proposed approach we have implemented simple neuron geometrries to construct

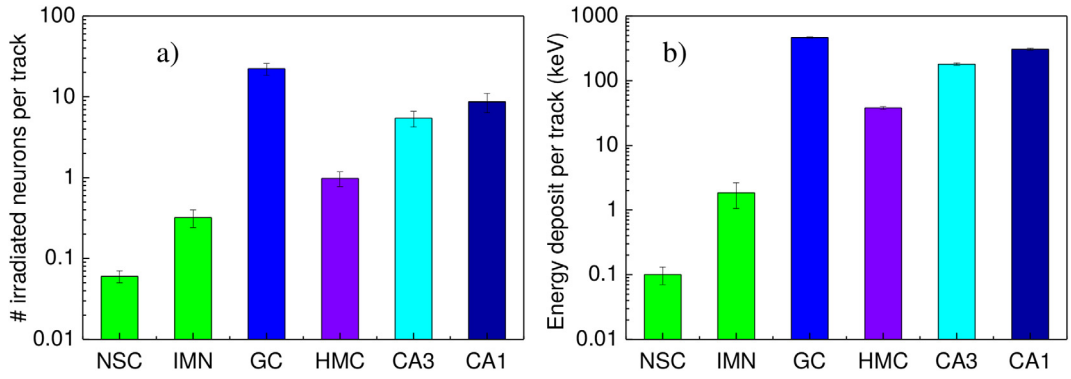

Fig. 5. Mean number of irradiated neurons in different regions of the rat hippocampus following exposure to a single ^{56}Fe ion with energy of 600 MeV/u (a). Mean energy deposition in irradiated neurons by single track of 600 MeV/u ^{56}Fe ion (b).

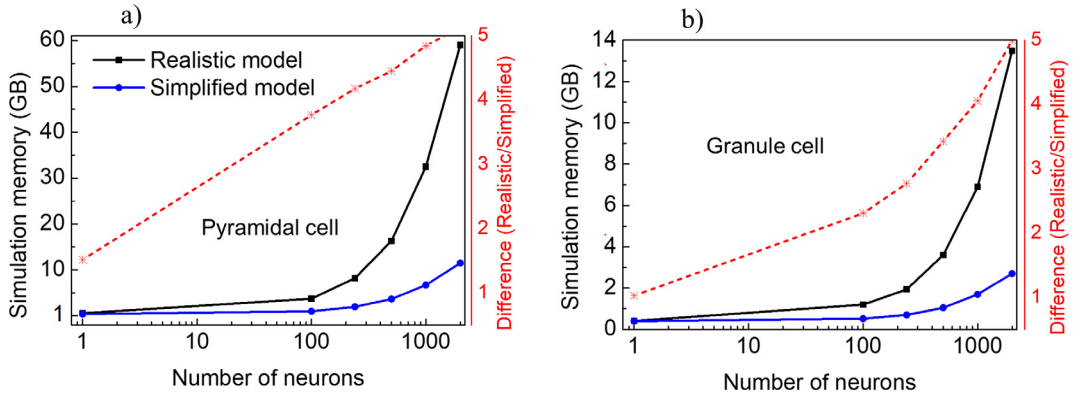

Fig. 6. Total amount of operative memory used for the Monte-Carlo track simulation under the irradiation of 600 MeV/u ^{56}Fe ions with fluence $3.2{\cdot}10^5$ particles/cm^2 in neural networks composed of realistic and simplified models of pyramidal (a) and granule cells (b). Red curves show ratio between memory usage for realistic and simplified models.

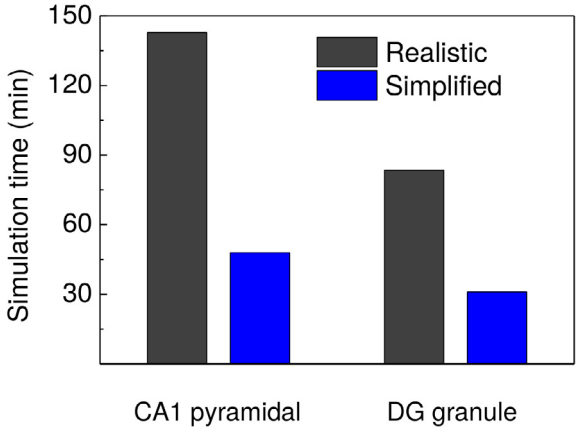

Fig. 7. Processor time used for the simulation of energy depositions following irradiation of neural network composed of realistic or simplified models of pyramidal and granule cell irradiated with 600 MeV/u ^{56}Fe ions with fluence $3.2{\cdot}10^5$ particles/cm^2. Both CA1 and DG neural networks contained 100 neurons.

the model of the rat hippocampus scaled about 1:100 with respect to real structure, and computed mean energy deposition in irradiated neurons of different types following single track of 600 MeV/u ^{56}Fe ion. Throughout the total number of 19367 neurons the most probable target was presented by dense population of granular cells in DG. However, we should stress that small population of radiosensitive neural stem cells and immature neurons, which is less than a percent of the total amount of neurons in hippocampus, could be of great importance for modeling of radiation-induced neurogenesis impairments [28]. Also, damage or loss of mossy cells in hippocampus is known to be responsible for the network disinhibition and increased risk of epileptic disorders [29]. Modeling of sufficient amount of these cells is a challenge in computational neuroscience of hippocampus [30].

Evidently, the understanding of processes leading to the final functional CNS impairments at the level of behavior and cognition should start from the quantatitative measures of energy depositions throughout the neuron components (soma, dendrites, spines, etc), for the number of cells with different morphology and spatial position. Therefore presented approach aims to present the initial conditions for the models considering specific types of radiation damage. For example, phenomenological models of neuron degradation [14] and neurogenesis impairments [28] strongly depend on particle type and radiation dose. Further development of related models would require knowledge about the spatial dose distributions in cells of different morphology or from different brain structures which can be provided by our approach.

Recent advances in Geant4-DNA-based computation of direct and indirect DNA damage [31–33] open prospects for their application to neurons. Developed model of hippocampus could be directly used to study distribution of DNA lesions throughout the cells of different morphology and spatial position.

Also, understanding of radiation-induced electrophysiology alterations could benefit from our models, which correctly represent electric parameters of the cells and can be incorporated in large-scale networks. Presently there is a lack of any consistent theoretical approaches linking this parts together. However, from the point of experiment analysis this may be methodically useful. Recently, there was an attempt to simulate the impact of experimentally observed electrophysiology alterations in a single neurons on the neural network activity [34]. The knowledge about the initial dose distribution and experimentally determined molecular effects (e.g. ion channels, membranes, synapses) could be further extrapolated to a sort of phenomenological model.

At the current state developed approach could provide the initial conditions for the models considering specific types of radiation damage. We hope that development of such biophysical models linking radiation damage and neuron function alteration could be achieved in near future.

Acknowledgements

This work was conducted as a part of the joint research between the Laboratory of Radiation Biology of Joint Institute for Nuclear Research and the National University of Mongolia. The authors acknowledge the financial support from JINR AYSS Grant (No. 18-702-02) and Russian Foundation for Basic Research (Grant No. 17-29-01007).

References

[1] Grigoryev AI, Krasavin EA, Ostrovsky MA. On the evaluation of the risk of the biological action of galactic heavy ions during an interplanetary flight. Russ J Physiol 2013;99:273.
[2] Parihar VK, Allen B, Tran KK, Macaraeg TG, Chu EM, Kwok SF, et al. What happens to your brain on the way to Mars. Sci Adv 2015;1:e1400256 .
[3] Sapetsky AO, Ushakov IB, Sapetsky NV, Shtemberg AS, Kositsin NS, Timofeev NN. Radiation neurobiology of long-term spaceflights. Biol Bull Rev 2017;7:443.
[4] Wu PH, Coultrap S, Pinnix C, Davies KD, Tailor R, Ang KK, et al. Radiation induces acute alterations in neuronal function. PloS ONE 2012;7:e37677 .
[5] Vlkolinsky R, Titova E, Krucker T, Chi BB, Staufenbiel M, Nelson GA, et al. Exposure to ^{56}Fe-particle radiation accelerates electrophysiological alterations in the hippocampus of APP23 transgenic mice. Radiat Res 2010;173:342.
[6] Machida M, Lonart G, Britten RA. Low (60 cGy) doses of ^{56}Fe HZE-particle radiation lead to a persistent reduction in the glutamatergic readily releasable pool in rat hippocampal synaptosomes. Radiat Res 2010;174:618.
[7] Greene-Schloesser D, Robbins ME, Peiffer AM, Shaw EG, Wheeler KT, Chan MD. Radiation-induced brain injury: a review. Front Oncol 2012;2:73.
[8] Rabin BM, Joseph JA, Hunt WA, Dalton TB, Kandasamy SB, Harris AH, et al. Behavioral endpoints for radiation injury. Adv Sp Res 1994;14:457.
[9] Rapp PR, Gallagher M. Preserved neuron number in the hippocampus of aged rats

with spatial learning deficits. Proc Natl Acad Sci 1996;93:9926.
[10] Batmunkh M, Belov OV, Bayarchimeg L, Lhagva O, Sweilam NH. Estimation of the spatial energy deposition in CA1 pyramidal neurons under exposure to 12C and 56Fe ion beams. J Radiat Res Appl Sci 2015;8:498.
[11] Alp M, Parihar VK, Limoli CL, Cucinotta FA. Irradiation of neurons with high-energy charged particles: an in silico modeling approach. PLoS Comput Biol 2015;11:e1004428 .
[12] Belov OV, Batmunkh M, Incerti S, Lkhagva O. Radiation damage to neuronal cells: simulating the energy deposition and water radiolysis in a small neural network. Phys Med 2016;32:1510.
[13] Batmunkh M, Belov OV, Bayarchimeg L, Lkhagva O. Radiation effects in the central nervous system: simulation technique and practical applications. Mong J Phys 2016;2:317.
[14] Alp M, Cucinotta FA. Biophysics model of heavy-ion degradation of neuron morphology in mouse hippocampal granular cell layer neurons. Radiat Res 2018;189:312.
[15] Ascoli GA, Donohue DE, Halavi M. NeuroMorpho.Org: a central resource for neuronal morphologies. J Neurosci 2007;27:9247.
[16] Desmond NL, Levy WB. Granule cell dendritic spine density in the rat hippocampus varies with spine shape and location. Neurosci Lett 1985;54:219.
[17] Gould E, Allan MD, McEwen BS. Dendritic spine density of adult hippocampal pyramidal cells is sensitive to thyroid hormone. Brain Res 1990;525:327.
[18] Papa M, Bundman MC, Greenberger V, Segal M. Morphological analysis of dendritic spine development in primary cultures of hippocampal neurons. J Neurosci 1995;15:1.
[19] Belly A, Bodon G, Blot B, Bouron A, Sadoul R, Goldberg Y. CHMP2B mutants linked to frontotemporal dementia impair maturation of dendritic spines. J Cell Sci 2010;123:2943.
[20] Carnevale NT, Hines ML. The NEURON book. New York: Cambridge University Press; 2005.
[21] Ropireddy D, Bachus SE, Ascoli GA. Non-homogeneous stereological properties of the rat hippocampus from high-resolution 3D serial reconstruction of thin histological sections. NSC 2012;205:91–111.
[22] Andersen P, Morris R, Amaral D, Bliss T, O'Keefe J. The hippocampus book. New York: Oxford University Press; 2007.
[23] Incerti S, Baldacchino G, Bernal M, Capra R, Champion C, Francis Z, et al. The Geant4-DNA project. Int J Model Simul Sci Comput 2010;1:157–78.
[24] Incerti S, Ivanchenko A, Karamitros M, Mantero A, Moretto P, Tran HN, et al. Comparison of Geant4 very low energy cross section models with experimental data in water. Med Phys 2010;37:4692–708.
[25] Bernal MA, Bordage MC, Brown JMC, Davidkova M, Delage E, Bitar ZE, et al. Track structure modeling in liquid water: a review of the Geant4-DNA very low energy extension of the Geant4 Monte Carlo simulation toolkit. Phys Med 2015;31:861–74.
[26] Incerti S, Kyriakou I, Bernal MA, Bordage MC, Francis Z, Guatelli S, et al. Geant4-DNA example applications for track structure simulations in liquid water: a report from the Geant4-DNA project. Med Phys 2018;45:e722–39.
[27] Curtis SB, Vazquez ME, Wilson JW, Atwell W, Kim M, Capala J. Cosmic ray hit frequencies in critical sites in the central nervous system. Adv Sp Res 1998;22:197.
[28] Cacao E, Cucinotta FA. Modeling heavy-ion impairment of hippocampal neurogenesis after acute and fractionated irradiation. Radiat Res 2016;186:624–37.
[29] Santhakumar V, Aradi I, Soltesz I. Role of mossy fiber sprouting and mossy cell loss in hyperexcitability: a network model of the dentate gyrus incorporating cell types and axonal topography. J Neurophysiol 2005;93:437.
[30] Schneider CJ, Bezaire M, Soltesz I. Toward a full-scale computational model of the rat dentate gyrus. Front Neural Circuits 2012;6:83.
[31] de la Fuente Rosales L, Incerti S, Francis Z, Bernal MA. Accounting for radiation-induced indirect damage on DNA with the Geant4-DNA code. Phys Med 2018;51:108–16.
[32] Lampe N, Karamitros M, Breton V, Brown JMC, Kyriakou I, Sakata D, et al. Mechanistic DNA damage simulations in Geant4-DNA part 1: A parameter study in a simplified geometry. Phys Med 2018;48:135–45.
[33] Lampe N, Karamitros M, Breton V, Brown JMC, Sakata D, Sarramia D, et al. Mechanistic DNA damage simulations in Geant4-DNA part 2: electron and proton damage in a bacterial cell. Phys Med 2018;48:146–55.
[34] Sokolova IV, Schneider CJ, Bezaire M, Soltesz I, Vlkolinsky R, Nelson GA. Proton radiation alters intrinsic and synaptic properties of CA1 pyramidal neurons of the mouse hippocampus. Radiat Res 2015;183:208.